

Structural modification of As–Se amorphous films

Oleg Luksha, Valentin Ivanitsky and Sergey Kolinko

Physical Department, Uzhgorod State University, 46 Gorky Street, 294000 Uzhgorod, USSR

Received 1 March 1990

Revised manuscript received 23 July 1991

The structure of $\text{As}_x\text{Se}_{100-x}$ amorphous films has been investigated by the radial distribution function method. Depending on the composition and preparation conditions, the short-range order of thin films is described by the model of chemically disordered network consisting of different $\text{SeSe}_{k/2}\text{As}_{(2-k)/3}$, $\text{AsSe}_{n/2}\text{As}_{(3-n)/2}$ structural units, where $k = 0, 1, 2$, $n = 0, 1, 2, 3$ and $\text{Se}=\text{AsSe}_{3/2}$ structural units have a double bond. A determining effect of the evaporation temperature of the initial glass upon the degree of middle-range order of films in the As–Se system has been shown. With annealing, the structural transformations with disappearance of the first sharp diffraction peak have been revealed.

1. Introduction

The structure of arsenic–chalcogen non-crystalline semiconductors has been studied by many authors (see reviews in refs. [1,2], and refs. therein). A large fraction of these works have been performed on materials of As–S systems, whereas the fraction concerned with their structure is limited (except for elementary Se). Less attention has been to the structure of $\text{As}_x\text{Se}_{100-x}$ amorphous films [2–7]. In the works cited, a thorough structural investigation has been made only for films with compositions $40 \leq x \leq 50$. The structure of the films with compositions $x < 40$ has been studied for some film materials with $x = 28.6$ [6], and $x = 5$, $x = 25$ and $x = 35$ [7].

For the first group of $\text{As}_x\text{Se}_{100-x}$ film compositions, the two main models of their amorphous structure have been proposed: the layered structure model [5] and cluster model [2–4]. Following the layered structure model, the disordered structure of films is built of ‘corrugated’ two-dimensional layers similar to those in As_2Se_3 crystal structure. Also, according to the cluster model the non-crystalline structure of films is supposed to be formed on the basis of ‘mixture’ of arsenic, selenium and arsenic selenide molecular units

(As_4 , Se_4 , As_2Se_3 , As_4Se_4 , As_2Se_4 , As_4Se_3 , As_2Se_2 etc.) with differing degrees of polymerization.

The papers in which models of the amorphous structure of films with $x \leq 40$ are proposed are not known to us. Leadbetter et al. showed [6] that $\text{As}_x\text{Se}_{100-x}$ vacuum-evaporated films possessed a very complicated structure which relaxed to the structure of the glasses with the same composition when annealed.

In ref. [7], the radial distribution function obtained from electron diffraction data provides the short-range order parameters of $\text{As}_x\text{Se}_{100-x}$ films for compositions with $x < 40$ only. An analysis of their structural peculiarities is missing.

The composition-dependent structural peculiarities of As–Se amorphous films are also characteristic of As–S films. Besides, the non-crystalline structure and properties of vacuum-evaporated films have been found by many investigators to be dependent on their preparation conditions. This dependence is explained by the formation of different structural states that can exist in an amorphous substance with a given chemical composition. For a generalized definition of this phenomenon, the term ‘structural modification’ is often used [8].

The aims of this work are two-fold. The first is to present a detailed investigation of the structure of $\text{As}_x\text{Se}_{100-x}$ amorphous films over the range of compositions with $x < 40$. The second is to analyze the potential of both models used together or independently to describe the disordered structure.

It should be noted that, in investigations performed elsewhere [2–7], the $\text{As}_x\text{Se}_{100-x}$ amorphous films were prepared by the convention thermal evaporation method at comparatively low evaporation temperatures. Therefore, we extended our analysis to study the structural modification of As-Se amorphous films when using the flash evaporation method with the higher evaporation temperatures.

2. Experimental

$\text{As}_x\text{Se}_{100-x}$ bulk glasses were prepared by the usual melt-quenching technique. The constituent elements, As and Se, were weighed and sealed in an evacuated (at 5×10^{-5} Torr) quartz ampoule which was placed in a furnace and heated stepwise at 700 K (8 h) 900 K (10 h) and 1050 K (15 h). The molten alloy was then quenched in air and the alloy was taken out by cutting the ampoule.

The initial vitreous alloys were powdered and separated according to sizes. Particles with an average size 200–300 μm were selected for evaporation. Thin films of different compositions of $\text{As}_x\text{Se}_{100-x}$ ($10 \leq x \leq 55$) were prepared by the flash evaporation method. The vacuum installation used was equipped with a device for uniform and controlled powder delivery into an open-type niobium evaporator. The evaporator temperature was measured with Pt–Pt–Rh thermocouple. The experiments on films evaporation were carried out at two values of the evaporator temperature, $T_{e1} = 770$ K and $T_{e2} = 870$ K. These values were within an experimentally selected range of evaporator temperatures in which flash evaporation conditions were realized. The other parameters were held at constant values: the substrate temperature, $T_s = 290$ K; condensation rate, $V_c = 5$ nm/s; the angle of molecular beam incidence

onto the substrate, $\phi = 30^\circ$; gas pressure, $P = 6 \times 10^{-3}$ Pa. Deposition was carried out onto glass substrates and freshly cleaved NaCl single crystals on the (001) plane. The chemical film composition was checked by an X-ray spectral microprobe (EMMA-4) method with a relative error $\pm 1\%$. The atomic film structure and its changes were investigated by the electron diffraction method with accelerating voltage $U = 75$ keV. Changes in structure of the films with thermal annealing were investigated in situ, in the electron diffractometer column (EMR-100). The film heating rate was varied within the limits of $V_h = 0.03$ to 0.64 K/s.

The dependence of the diffracted electron beam intensity $I = f(s)$, where $s = 4\pi \sin \theta / \lambda$, θ = diffraction angle and λ = wavelength of electrons, was plotted in the direct electronic current recording mode. Short-range order parameters of the atomic film structure were obtained by calculating the radial distribution functions (RDF) in compliance with the procedure as reported earlier in refs. [9,10]. For electron diffraction studies, the typical thickness of the films was 50–60 nm. Films were separated from NaCl substrate and located onto a copper grid with 200 μm mesh. The necessary values of amorphous film density for the RDF calculation were determined by measuring the mass and volume of the layers varying in thickness between 1.5 and 3.5 μm . The thickness of the films was determined very accurately by the interference method with a mean error ± 0.02 μm ; the masses of the films were measured by direct weighing with a mean error $\pm 10^{-5}$ g. When the density of films was determined, its mean relative error was $\pm 2\%$. The data about the changes in the medium-range order of the atomic film structure were measured by the analysis of the first sharp peak positions and intensity of the diffraction patterns.

3. Results

The investigations were carried out with $\text{As}_x\text{Se}_{100-x}$ amorphous films for stated compositions ($x = 10, 20, 30, 40, 47$ and 55). X-ray spectral microprobe data justified an excellent fitness

The aims of this work are two-fold. The first is to present a detailed investigation of the structure of $\text{As}_x\text{Se}_{100-x}$ amorphous films over the range of compositions with $x < 40$. The second is to analyze the potential of both models used together or independently to describe the disordered structure.

It should be noted that, in investigations performed elsewhere [2–7], the $\text{As}_x\text{Se}_{100-x}$ amorphous films were prepared by the convention thermal evaporation method at comparatively low evaporation temperatures. Therefore, we extended our analysis to study the structural modification of As–Se amorphous films when using the flash evaporation method with the higher evaporation temperatures.

2. Experimental

$\text{As}_x\text{Se}_{100-x}$ bulk glasses were prepared by the usual melt-quenching technique. The constituent elements, As and Se, were weighed and sealed in an evacuated (at 5×10^{-5} Torr) quartz ampoule which was placed in a furnace and heated stepwise at 700 K (8 h) 900 K (10 h) and 1050 K (15 h). The molten alloy was then quenched in air and the alloy was taken out by cutting the ampoule.

The initial vitreous alloys were powdered and separated according to sizes. Particles with an average size 200–300 μm were selected for evaporation. Thin films of different compositions of $\text{As}_x\text{Se}_{100-x}$ ($10 \leq x \leq 55$) were prepared by the flash evaporation method. The vacuum installation used was equipped with a device for uniform and controlled powder delivery into an open-type niobium evaporator. The evaporator temperature was measured with Pt–Pt–Rh thermocouple. The experiments on films evaporation were carried out at two values of the evaporator temperature, $T_{e1} = 770$ K and $T_{e2} = 870$ K. These values were within an experimentally selected range of evaporator temperatures in which flash evaporation conditions were realized. The other parameters were held at constant values: the substrate temperature, $T_s = 290$ K; condensation rate, $V_c = 5$ nm/s; the angle of molecular beam incidence

onto the substrate, $\phi = 30^\circ$; gas pressure, $P = 6 \times 10^{-3}$ Pa. Deposition was carried out onto glass substrates and freshly cleaved NaCl single crystals on the (001) plane. The chemical film composition was checked by an X-ray spectral microprobe (EMMA-4) method with a relative error $\pm 1\%$. The atomic film structure and its changes were investigated by the electron diffraction method with accelerating voltage $U = 75$ keV. Changes in structure of the films with thermal annealing were investigated in situ, in the electron diffractometer column (EMR-100). The film heating rate was varied within the limits of $V_h = 0.03$ to 0.64 K/s.

The dependence of the diffracted electron beam intensity $I = f(s)$, where $s = 4\pi \sin \theta / \lambda$, θ = diffraction angle and λ = wavelength of electrons, was plotted in the direct electronic current recording mode. Short-range order parameters of the atomic film structure were obtained by calculating the radial distribution functions (RDF) in compliance with the procedure as reported earlier in refs. [9,10]. For electron diffraction studies, the typical thickness of the films was 50–60 nm. Films were separated from NaCl substrate and located onto a copper grid with 200 μm mesh. The necessary values of amorphous film density for the RDF calculation were determined by measuring the mass and volume of the layers varying in thickness between 1.5 and 3.5 μm . The thickness of the films was determined very accurately by the interference method with a mean error ± 0.02 μm ; the masses of the films were measured by direct weighing with a mean error $\pm 10^{-5}$ g. When the density of films was determined, its mean relative error was $\pm 2\%$. The data about the changes in the medium-range order of the atomic film structure were measured by the analysis of the first sharp peak positions and intensity of the diffraction patterns.

3. Results

The investigations were carried out with $\text{As}_x\text{Se}_{100-x}$ amorphous films for stated compositions ($x = 10, 20, 30, 40, 47$ and 55). X-ray spectral microprobe data justified an excellent fitness

of the chemical film composition to that of initial glasses that additionally testified to flash evaporation conditions being observed.

The RDFs of $\text{As}_x\text{Se}_{100-x}$ as-deposited amorphous films prepared at T_{e1} and T_{e2} are shown in figs. 1 and 2, respectively. Table 1 contains the values of coordination sphere radii and under peak areas.

$\text{As}_{20}\text{Se}_{80}$ films evaporated at T_{e1} and T_{e2} , and $\text{As}_{30}\text{Se}_{70}$ films at T_{c1} have different a type the structure. The RDF analysis gives the following average values of coordination sphere radii for them: $r_1 = 2.05 \text{ \AA}$, $r'_1 = 2.75 \text{ \AA}$, $r_2 = 3.65 \text{ \AA}$, $r'_2 = 4.44 \text{ \AA}$.

The electron diffraction patterns of all the investigated as-deposited $\text{As}_x\text{Se}_{100-x}$ amorphous films revealed a sharp peak (FSDP) in the region of $s \approx 10 \text{ nm}^{-1}$. The availability of the medium-range order in the amorphous substance is usually related to it. For comparative analysis of the diffraction patterns, we plotted I/I_0 curves, where I and I_0 are the intensities $I = f(s)$ and the second peak of the diffraction patterns, respectively. I/I_0 curves of $\text{As}_{40}\text{Se}_{60}$ as-deposited films obtained at T_{e1} and T_{e2} (curves 1 and 2, respectively), and annealed films (curve 3) are shown in fig. 3. The composition dependences of

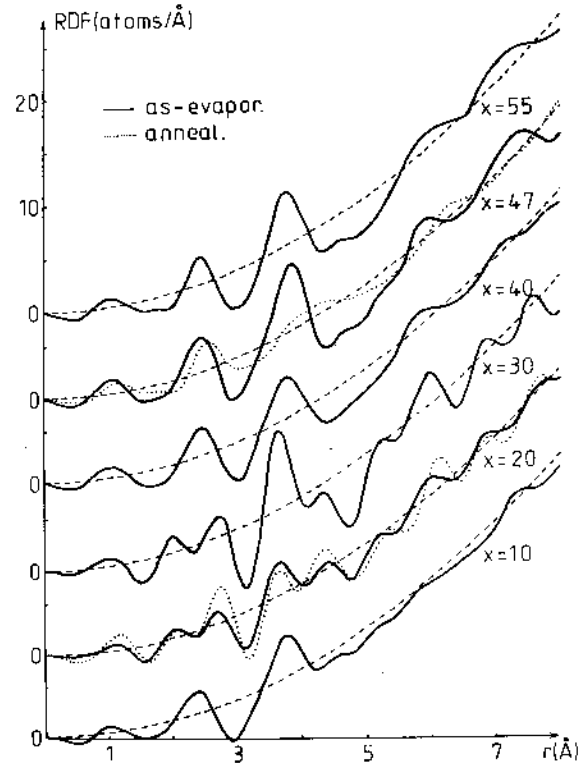


Fig. 1. The RDF of $\text{As}_x\text{Se}_{100-x}$ as-deposited (full line) and annealed films (dotted lines) prepared at $T_{c1} = 770 \text{ K}$. The dashed lines indicate average atomic density of films.

Table 1
The RDF parameters for $\text{As}_x\text{Se}_{100-x}$ amorphous films

Film composition	T_c (K)	RDF maxima positions				Under-peak areas (arbitrary units)		
		r_1 (Å)	r'_1 (Å)	r_2 (Å)	r'_2 (Å)	b_1	b'_1	b_2
$\text{As}_{10}\text{Se}_{90}$	770	2.40	—	3.75	—	2.4	—	8.8
	870	2.45	—	3.85	—	3.1	—	10.1
$\text{As}_{20}\text{Se}_{80}$	770	2.05	2.70	3.60	4.40	1.1	1.5	4.9
	870	2.10	2.80	3.65	4.50	1.5	1.7	5.9
$\text{As}_{30}\text{Se}_{70}$	770	2.00	2.70	3.60	4.30	1.1	1.5	6.1
	870	2.40	—	3.70	—	2.4	—	8.2
$\text{As}_{40}\text{Se}_{60}$	770	2.45	—	3.75	—	3.0	—	7.9
	870	2.40	—	3.75	—	3.1	—	8.9
$\text{As}_{47}\text{Se}_{53}$	770	2.40	—	3.80	—	2.9	—	9.6
	870	2.40	—	3.65	—	3.1	—	7.0
$\text{As}_{55}\text{Se}_{45}$	770	2.45	—	3.80	—	2.3	—	8.8
	870	2.45	—	3.75	—	2.6	—	7.4

T_e , evaporation temperature; r , coordination sphere radii; b , under-peak area of the RDF.

intensity I_1/I_0 of the first diffraction peak are shown for as-deposited $\text{As}_x\text{Se}_{100-x}$ films in fig. 4, curves 1 (T_{e1}) and 3 (T_{e2}). These dependences after 3–4 h film relaxation under usual conditions (curves 2 and 4 for T_{e1} and T_{e2} , respectively) are shown in the same figure. The increase in the evaporation temperature from T_{e1} to T_{e2} considerably increases the intensity of the first peak for the films with compositions $x = 30, 40, 47$ and decreases it for the films with $x = 10, 20, 55$. At structural relaxation of layers under natural aging conditions, the character of composition dependences I_1/I_0 remains the same. However, depending on the composition and evaporation temperature, T_e , of films, both the increase and decrease in I_1/I_0 at relaxation is observed. If the I_1/I_0 parameter directly represents the degree of the medium-range order to be realized in films,

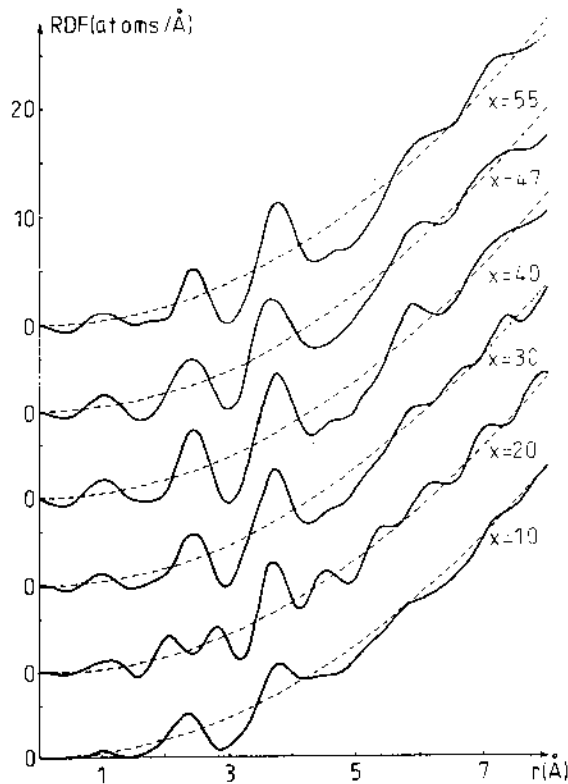


Fig. 2. The RDF of $\text{As}_x\text{Se}_{100-x}$ as-deposited amorphous films prepared at $T_{e2} = 870$ K. The dashed lines indicate average atomic density of films.

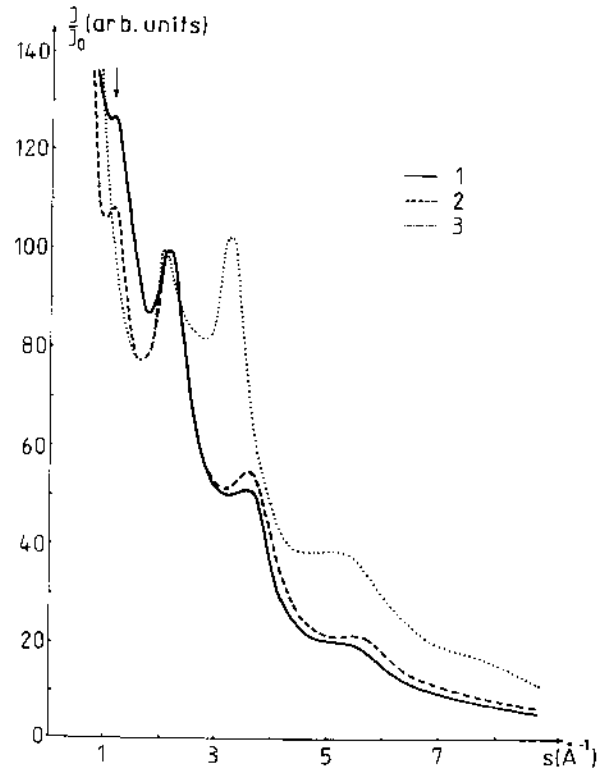


Fig. 3. Diffraction patterns of $\text{As}_{40}\text{Se}_{60}$ amorphous films: deposited at $T_{e1} = 770$ K (curve 1), at $T_{e2} = 870$ K (curve 2) and annealed (curve 3).

the above relationships characterize just the change in the medium-range order of $\text{As}_x\text{Se}_{100-x}$ films while varying their composition, T_e and structural relaxation.

The thermal annealing in vacuum of all the investigated $\text{As}_x\text{Se}_{100-x}$ amorphous films at temperatures lower than some limiting values of T_0 led to the stimulation of relaxation processes in the film structure. The peak intensities in the diffraction patterns and the RDF parameters of layers changed insignificantly. Heating of films above temperature T_0 caused a threshold structural transformation in them, amorphicity of structure remaining the same. During such a transformation, the FSDP disappeared completely in the diffraction pattern; the positions and intensities of the subsequent diffraction curve peaks (fig. 3) changed. The electron microscopic investigations showed that during such structural

transformation an absorption contrast in the film image changed significantly, too (fig. 5). In the initial 'bright' film near the edges of the grid-holder, there appeared areas of 'darker' contrast in the film which suffered from the structural transformation. The boundary between 'bright' and 'dark' areas is always sharp. During structural transformation, it shifts to the centre of the mesh of the grid-holder at speed dependent on the initial film structure and annealing temperature $T \geq T_0$. After structural transformation, a total film becomes relatively 'dark' by contrast. So, the structural transformation is irreversible. The subsequent heating of the film to the higher

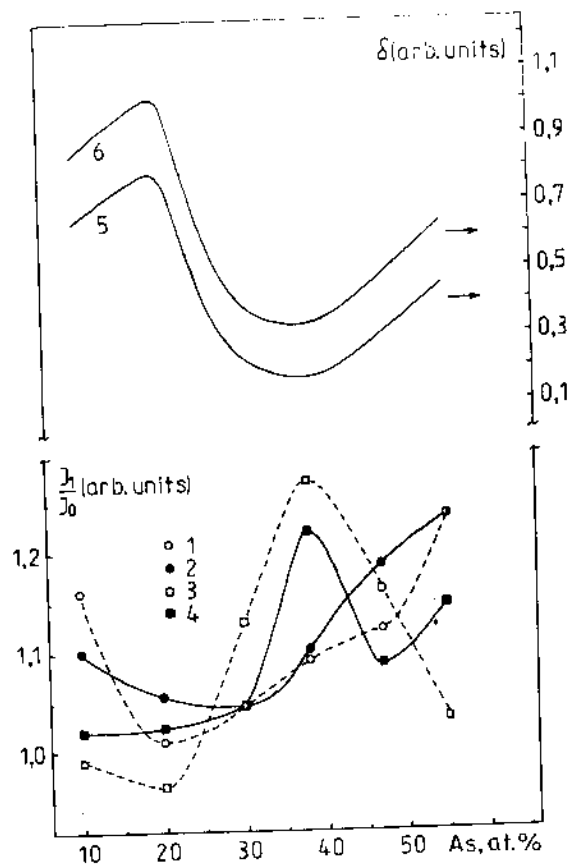


Fig. 4. Intensities, I_1/I_0 , of the first diffraction, sharp peak for $\text{As}_x\text{Se}_{100-x}$ amorphous films: as-deposited at $T_{\text{el}} = 870$ K (1) and after natural aging (2); as-deposited films at $T_{\text{c2}} = 770$ K (3) and after natural aging (4). In the upper part, the dependence of the degree of vapour 'overheating', δ , for T_{el} (5) and T_{c2} (6) is given.

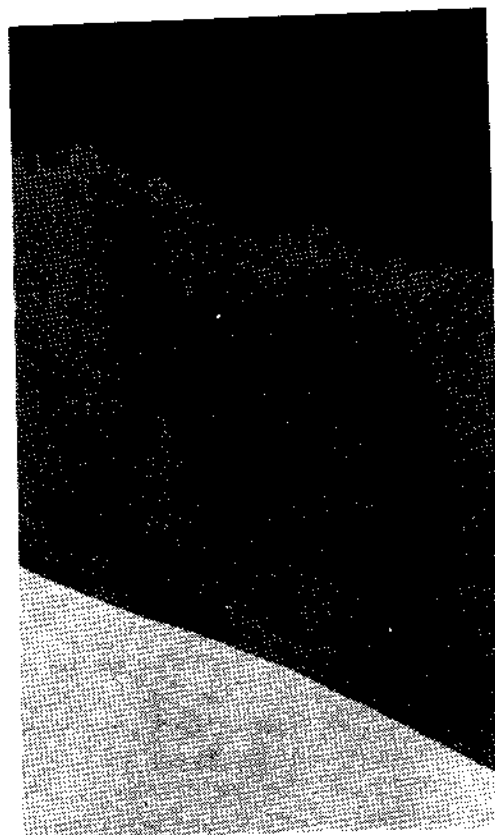


Fig. 5. Typical electron microphotograph ($\times 1650$) of the $\text{As}_{40}\text{Se}_{60}$ amorphous film when heated, taken during the structural transformation. The edge of the objective microscope grid (black field) and accompanying phase states of the film are to be seen: initial film (bright contrast, diffraction pattern 2 in fig. 3) and the film after transformation (the darker contrast, diffraction pattern 3 in fig. 3).

temperatures does not cause significant structural changes in it up to the onset of crystallization. The values of temperature T_0 for the structural transformation onset of $\text{As}_x\text{Se}_{100-x}$ films are within the range of 375–445 K. A pronounced T_0 dependence of the film composition is not revealed. At the same time, a significant effect of the layer prehistory upon the value of T_0 can be seen. $\text{As}_{40}\text{Se}_{60}$ films are the most stable to the structural transformation ($T_0 \approx 430$ K).

$\text{As}_{10}\text{Se}_{90}$ films are the least stable ($T_0 \approx 335$ K). The film heating rate from 0.03 K/s to 0.64 K/s increased the average values of T_0 for 15–45

K at dynamic annealing depending on the composition.

4. Discussion

4.1. Short-range order structural modification

The RDF analysis shows that, irrespective of the value of T_e , the parameters of the short-range structure order of films with compositions $x = 10, 40, 47, 55$ are close to those for bulk glasses [11,12] and for layers of the As–Se system prepared by a conventional thermal evaporation method [7,13]. Average values of coordination sphere radii are equal to $\bar{r}_1 = 2.40 \text{ \AA}$ and $\bar{r}_2 = 3.75 \text{ \AA}$. Taking into account these data, the short-range order of the atomic film structure is well described by the model of chemically disordered network consisting of $\text{SeSc}_{k/2}\text{As}_{(2-k)/3}$ and $\text{AsSe}_{n/2}\text{As}_{(3-n)/3}$ structural units, where $k = 0, 1, 2$; $n = 0, 1, 2, 3$. The ratio and character of correlation of different structural units in an amorphous layer structure are defined by its chemical composition, preparation conditions and subsequent external factors.

The covalent radii values of As (1.18 \AA) and Se (1.14 \AA) are close to each other [14]. Therefore, the change in the ratio of stated structural units should not produce an appreciable change in the values of r_1 . The angles between covalent bonds around As and Se bonds may change depending on the ratio of structural units (at $r_1 \approx \text{const.}$), pre-determining noticeable changes in r_2 . In the above structural units, the number of the nearest neighbours around an As atom is equal to 3, and for Se atom it is equal to 2; therefore the change in the ratio of the structural units in a film considerably changes the values b_1 and b_2 . The experimental results given in table 1 are in excellent agreement with the relationships pointed out and confirm, indirectly, the reality of the proposed structure model for $\text{As}_x\text{Se}_{100-x}$ amorphous films with compositions $x = 10, 40, 47, 55$. To define the ratio of different structural units in amorphous films, additional investigations are still underway using the proposed [15] method. For $\text{As}_{20}\text{Se}_{80}$ films, since $r_1 = 2.05 \text{ \AA}$ differs greatly

from the sum of covalent radii for As and Se atoms, we suppose that this value of r_1 corresponds to the double bonding length [16]. Taking into account that the relevant coordination number for $\text{As}_{20}\text{Se}_{80}$ and $\text{As}_{30}\text{Se}_{70}$ films is close to unity, the mean statistic atom to be chosen as a count-off point will form a double bond with one atom only.

Structural units with one double bond are revealed [1] in non-crystalline oxides, phosphorus sulphides and selenides (structural units of $\text{Se=PSc}_{3/2}$ type) and As_2S_5 amorphous films ($\text{S=AsS}_{3/2}$ type). For non-crystalline arsenic selenides, the experimental data serving as the basis for the description of the short-range structure in terms of the $\text{Se=AsSe}_{3/2}$ structural unit have been deficient [1]. Consequently a more careful justification is required for the introduction of a structural unit with a double bond.

A double bond between As and Se atoms has a length considerably smaller than that of a single bond. Besides, a repulsive interaction of double bonding electrons with single bonding ones around As atom in the $\text{Se=AsSe}_{3/2}$ structural unit produces some change in the parameters of single bonds [16]. Thus, in a $\text{Se=AsSe}_{3/2}$ structural unit, one should expect some increase in single bonding length compared with analogous bonds in $\text{AsSe}_{3/2}$ pyramid and the deflection of α and β

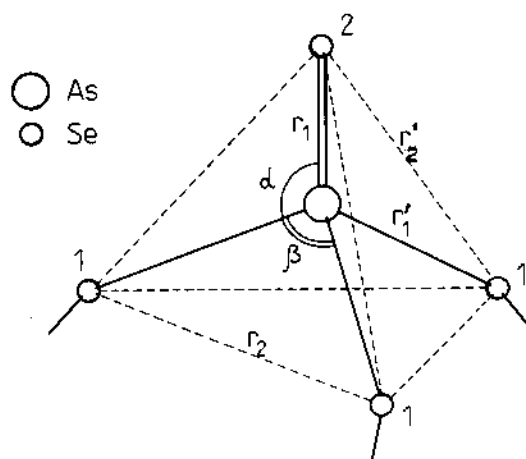


Fig. 6. Geometrical model of $\text{Se=AsSe}_{3/2}$ structural unit with double bond.

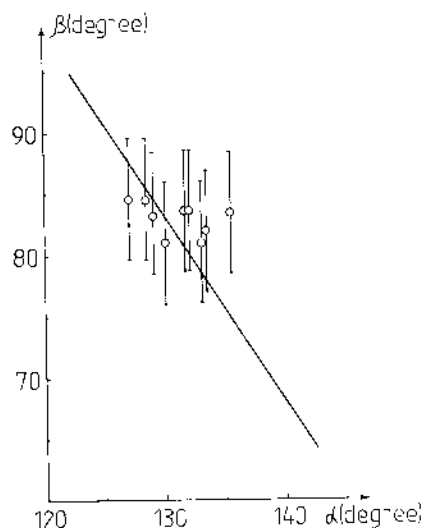


Fig. 7. Theoretical angular dependence (solid line) and points to be obtained according to the experimental data for angles α and β between directions of bonds in $\text{Se}=\text{AsSe}_{3/2}$ structural unit.

angles (fig. 6) from tetrahedral angles ($\alpha > 109.5^\circ > \beta$). With the help of the above argument, the position of the first RDF maximum, r_1 , of $\text{As}_{20}\text{Se}_{80}$ and $\text{As}_{30}\text{Se}_{70}$ amorphous films may be matched up with the double bonding length in $\text{As}=\text{AsSe}_{3/2}$ structural unit, r'_1 (with the mean single bonding length), r_2 (with the distance between two atoms Se_1 , and r'_2 (with the distance between Se_1 and Se_2 atoms). $\text{Se}=\text{AsSe}_{3/2}$ structural unit symmetry for interdependent α and β angles gives the relation $\sin(\beta/2) = \sqrt{3}/2 \sin(180^\circ - \alpha)$. A theoretical angular dependence and datapoints that are obtained using the experimental data are shown in fig. 7.

Thus, the experimental values of coordination sphere radii r_1 , r'_1 , r_2 , r'_2 agree fairly well with the model $\text{Se}=\text{AsSe}_{3/2}$ structural unit if $\alpha = 130^\circ$ and $\beta = 83^\circ$ are the mean angles. However, the values of areas under the peaks calculated for this model do not agree well with the experimental values.

One may considerably improve the quality of the fit between these values by introducing the model structure of such films together with $\text{Se}=\text{AsSe}_{3/2}$ and $\text{AsSe}_{3/2}$, $\text{SeSe}_{k/2}\text{As}_{(2-k)/3}$ structural units into the disordered network. The

reality of such supposition is confirmed by the absence of a well-defined separation of the RDF peaks at r_1 , r'_1 and r_2 , r'_2 . This lack of separation means that correlations in the location of atoms at the distances of 2.40 Å and 3.90 Å contribute also to the RDF which coincides with the first and second coordination sphere radii of $\text{AsSe}_{3/2}$ and $\text{SeSe}_{k/2}\text{As}_{(2-k)/3}$ structural units.

So, the short-range order of the atomic structure for $\text{As}_{20}\text{Se}_{80}$ (at T_{e1} and T_{e2}) and $\text{As}_{30}\text{Se}_{70}$ (at T_{e1} films) may be described by the model of a chemically disordered network consisting of $\text{Se}=\text{AsSe}_{3/2}$, $\text{AsSe}_{3/2}$ and $\text{SeSe}_{k/2}\text{As}_{(2-k)/3}$. We denote such films as those having a_2 -type amorphous structure. The ratio and character of correlation of the above structural units in the films with a_2 -type amorphous structure are also defined by the chemical composition, preparation and post-condensation aging conditions. That is why, these factors being changed, the short-range order structure of a_2 -type films may be greatly influenced. This fact finds its confirmation in the values of the RDF parameters (table 1). A simultaneous realization of several conditions may probably promote the formation of $\text{Se}=\text{AsSe}_{3/2}$ structural units in the disordered network of $\text{As}_{20}\text{Se}_{80}$ and $\text{As}_{30}\text{Se}_{70}$ films.

(1) Under flash evaporation conditions of the initial glass powder at $T_e = 770\text{--}870$ K, the atomic complexes which tend to form the $\text{As}=\text{Se}$ double bond exist in vapour. It should be noted that we failed to prepare the short-range structure films of a_2 -type by the conventional thermal evaporation method.

(2) The composition and structure of $\text{As}_{20}\text{Se}_{80}$ and $\text{As}_{30}\text{Se}_{70}$ glasses also promote the formation of particular atomic complexes in vapour phase during flash evaporation.

(3) The comparatively higher evaporation temperatures, T_e , are enough to excite the atomic complexes with subsequent electron orbital hybridization of As and Se atoms necessary for the formation of the structural units with double bonding.

(4) A low substrate temperature promotes quenching of $\text{Se}=\text{AsSe}_{3/2}$ structural units to be coordinated into the disordered network during film condensation.

4.2. Medium-range order structural modifications

Different explanations for the nature of the FSDP in non-crystalline substances have been proposed [17–22]. We give preference to the cluster model for amorphous films. Following this model the FSDP is conditioned by the availability of molecular and (or) quasimolecular structural species in the disordered network of $\text{As}_x\text{Se}_{100-x}$ films. The chemical composition, concentration and character of correlation of different molecular species in the disordered network are defined by the chemical composition of the film and its preparation conditions (see fig. 4).

The availability of different quasimolecular species in $\text{As}_x\text{Se}_{100-x}$ films is predetermined by the vapour phase composition when the initial glass is being evaporated [6,23]. Mass spectroscopic investigations of the vapour phase composition when arsenic selenides As_2Se_5 , As_2Se_3 and AsSe are evaporated [6] showed that in all the cases the vapour contained a number of different multi-atomic complexes. It should be noted that these investigations are carried out at the lower evaporation temperatures in comparison with melting temperatures for the corresponding arsenic selenides; therefore, the mass spectra, given in ref. [6], are probably associated with the sublimation process. However, we used evaporation temperatures which were 250 to 450 °C higher in our investigations. However, we assume that a substantial amount of multi-atomic complexes was present in vapour even at such evaporation temperatures. When vapour condenses onto the substrate, many of these complexes are connected into the disordered network of the amorphous film in the form of molecular and (or) quasimolecular species. The increase in the evaporation temperature of the substance increases the energy of vapour particles and decreases the concentration of multiatomic particles [24].

To analyze the results obtained on the influence of the evaporation temperature for the initial $\text{As}_x\text{Se}_{100-x}$ glass upon the FSDP intensity, we have calculated the degree of vapour ‘overheating’ with respect to its state at liquidus temperatures, T_L , for the As–Se system by the formula $\delta = (T_e - T_L)/T_L$. The values of T_L are

taken from ref. [25]. The concentration dependences of δ in the case of T_{e1} and T_{e2} are given in fig. 4 (curves 5 and 6, respectively). In the case of $T_{e1} = 770$ K, a full correlation of the composition dependences of the FSDP intensity and parameter δ for as-deposited films is observed: the increase in the degree of vapour overheating (the decrease in the concentration of multi-atomic complexes) corresponds to the increase of I_1/I_0 . The observed correlation of δ and I_1/I_0 testifies to a determining effect of the composition and energy of vapour phase particles upon the medium-range order of condensing $\text{As}_x\text{Se}_{100-x}$ amorphous films.

An increase of evaporation temperature to 870 K in the preparation of $\text{As}_x\text{Se}_{100-x}$ films causes a loss of correlation between δ and I_1/I_0 and composition, especially in the region of compositions $40 \leq x \leq 60$ (fig. 4, curve 6). This loss may be conditioned by: (a) more complex vapour phase composition dependence of the evaporation temperature of initial glass; (b) the initial glass composition and structure effect upon the vapour phase composition and its temperature dependence; (c) the formation of the middle-range order structural species not only from the multi-atomic vapour particles but from one, two, and three atomic particles during association on the substrate and connection to the growing films. The middle-range order formation mechanism in $\text{As}_x\text{Se}_{100-x}$ films is indirectly indicated by the fact that the increase in the middle-range order degree occurs in some films in the disordered structure already formed at structural relaxation (fig. 4, curves 1, 2 or 3, 4).

4.3. Structural changes at thermal annealing

The structural transformation of the medium-range order of the disordered film structure significantly changed the RDF and its parameters (fig. 1, dotted curves). In the case of a film with the short-range order structure of a_1 -type, the structure disordering at short-range increased drastically (fig. 1, RDF for $x = 47$). For films with short-range order structure of a_2 -type the first RDF peak remained practically unchanged after structural transformation, and the subsequent

peaks changed less than those of a_1 -type films (fig. 1, RDF for $x = 20$).

Many works have been devoted to the temperature dependence of the FSDP intensity [17,19,26–28]. It has been established that for well-annealed glasses and amorphous films an insignificant increase in the peak intensity with increasing temperature (abnormal behaviour) is observed. The annealing of as-deposited amorphous films decreases the FSDP intensity and the layer structure is close to that of glass [6,28]. The latter case is realized in $\text{As}_x\text{Se}_{100-x}$ films investigated by us.

We consider the model of ‘polymerization’ of molecular structural species into the more continuous disordered network [23,29] to be the most suitable one to explain the decrease in the FSDP intensity for as-deposited amorphous films after annealing [23,29]. Just preceding the ‘polymerization’ processes in the disordered network of $\text{As}_x\text{Se}_{100-x}$ as-deposited films for annealing above a temperature, T_0 , defines the change in structure to be observed in the form of the structural transformation described. During polymerization in the short-range structure of a_1 -type, the middle-range order decreases drastically and the nearest environment of the majority of atoms (fig. 1, $x = 47$) changes to some extent. In the case of the short-range structure of a_2 -type, the middle-range order also decreases drastically during polymerization, but the nearest atom environment changes less (fig. 1, $x = 20$). The strongest double bonds in $\text{Se}=\text{AsSe}_{3/2}$ structural units remain practically unchanged.

The structural transformations observed by us in as-deposited $\text{As}_x\text{Se}_{100-x}$ films differ from those observed earlier by a full disappearance of the FSDP in the diffraction patterns, i.e., in the films under investigation, the polymerization of molecular and (or) quasimolecular structural species into more uniform disordered network was fully completed after annealing within the range of temperatures, $T > T_0$. This disappearance is due to the peculiarity of thin film samples investigated by us. In all the works known to us, the structural changes have been studied in relatively thick layers ($\sim 0.5 \mu\text{m}$ thick) on different substrates. The initiation of thermally stimulated

structural transformations in the latter gives rise to internal mechanical stresses in the disordered atomic network of the film. At the stage of thermally stimulated structural changes (of polymerization processes), the stresses reach a level at which further structural transformations are not possible. As a result, the FSDP intensity of such films after annealing will correspond to a degree of polymerization which is related to the internal mechanical stresses in films.

We have investigated the $\text{As}_x\text{Se}_{100-x}$ self-supported thin films (50–60 nm) positioned on a grid-holder. Under such conditions the mechanical stresses which occur during thermally stimulated structural transformations may relax easily due to flexure of films. Indeed, an electron microscopic study, in situ, during thermally stimulated structural transformation processes showed local flexures, ‘dark’ areas, subjected to structural transformation (fig. 5) near boundaries with ‘light’ (initial) areas.

5. Conclusions

In the present work, it has been shown that, depending on the evaporation temperature of initial glasses in the As–Se system, different structure types are produced in $\text{As}_x\text{Se}_{100-x}$ thin films. The structure of films with $x = 10, 40, 47, 55$ prepared at evaporation temperatures of 770 and 870 K and with $x = 30$ prepared at 870 K is well described by the model of chemically disordered network consisting of $\text{SeSe}_{k/2}\text{As}_{(2-k)/3}$ and $\text{AsSe}_{n/2}\text{As}_{(3-n)/2}$ structural units where $k = 0, 1, 2, n = 0, 1, 2, 3$. In the films with $x = 20$ prepared at evaporation temperatures of 770 K and 870 K and with $x = 30$ prepared at 770 K, the unit $\text{Se}=\text{AsSe}_{3/2}$ with a double bond is the main structural unit which defines the short-range order.

A close correlation of the FSDP intensity of films and vapour overheating degree relative to the liquidus temperature at their deposition has been observed that testifies to a determining effect of the composition and energy of vapour phase particles upon the middle-range order of As–Se condensing amorphous films. Annealing $\text{As}_x\text{Se}_{100-x}$ self-supported films (500–600 Å)

above some threshold temperature, dependent, on x , the structural transformation with a full FSDP disappearance proceeds, while the amorphicity of structure remains the same.

References

- [1] A. Felts, *Amorphe und Glasartige Anorganische Festkörper* (Akademie-Verlag, Berlin, 1983).
- [2] V.P. Zakharov and V.S. Gerasimenko, *Strukturne osobennosti poluprovodnikov v amorfnom sostojanii* (Structural Peculiarities of Semiconductors in Amorphous State) (Naukova dumka, Kiev, 1967) p. 280.
- [3] S.B. Mamedov, V.G. Pogoreva and O.A. Yakovuk, in: *Proc. 4th All-Union Conf., Suzdal, 1984, Chernogolovka*, Vol. 2 (1984) 17.
- [4] T.N. Mamontova and A.V. Chernishev, *Sov. J. Phys. Techn. Semiconductors* 18 (1984) 536.
- [5] R.J. Nemanich, G.A.N. Connell, T.M. Hayes and R.A. Street, *Phys. Rev. B* 18 (1978) 6900.
- [6] A.J. Leadbetter, A.J. Apling and M.F. Danil, *J. Non-Cryst. Solids* 21 (1976) 47.
- [7] V.M. Kozlov and Yu.A. Ekmanis, in: *Sovremennay elektronnyy mikroskopiy v issledovanii veshchestva* (Modern Electronic Microscopy in Substance. Investigation), ed. B.B. Zvjagin (Nauka, Moscow, 1982) p. 159.
- [8] L.N. Blinov, M.D. Balmakov and N.S. Pocheptsova, *Lett. Sov. J. Techn. Phys.* 14 (1988) 86.
- [9] A.F. Skrishevsky, *Structural Analysis of Liquids and Amorphous Bodies* (Visshaya Shkola, Moscow, 1980) 328.
- [10] Yu.I. Stetsiv, *Sov. Crystallogr.* 18 (1973) 257.
- [11] Yu.G. Poltavtsev, *Struktura poluprovodnikovich rasplavov* (Structure of Semiconductor Melts) (Metallurgiya, Moscow, 1984) 176.
- [12] N.F. Mott and E.A. Davis, *Electron Processes in Non-Crystalline Materials*, 2nd Ed. (Clarendon, Oxford, 1979).
- [13] A.L. Renninger and B.L. Averbach, *Phys. Rev. B* 8 (1973) 1507.
- [14] G.B. Bokiy, *Kristalloyimiy* (Crystal Chemistry) (Nauka, Moscow, 1971) 400.
- [15] A.J. Alping, A.J. Leadbetter and A.C. Wright, *J. Non-Cryst. Solids* 23 (1977) 369.
- [16] K. Dey and D. Selbin, *Theoretical Non-Organic Chemistry* (trans. from English) (Khimiya, Moscow, 1976) 567.
- [17] L. Červinka, *Czechosl. J. Phys.* B35 (1985) and 1193.
- [18] S. Susman, D.L. Price, K.J. Volin, R.J. Dejus and D.G. Montague, *J. Non-Cryst. Solids* 106 (1988) 26.
- [19] S.R. Elliott, *J. Non-Cryst. Solids* 97&98 (1987) 159.
- [20] D.L. Price, S. Susman, K.J. Volin and R.J. Dejus, *Physica B* 156&157 (1989) 189.
- [21] S. Zannin Jeffrey, *Phys. Today* 41 (1988) 28.
- [22] D.L. Price, S.S. Moss, R. Reijers, M.-Z. Sabounji and S. Susman, *J. Phys. Condens. Matter* 1 (1988) 1005.
- [23] D.J. Freacy, U. Strom, P.B. Klein, R.C. Taylor and T.P. Martin, *J. Non-Cryst. Solids* 35&36 (1980) 1035.
- [24] A.S. Pashinkin and A.S. Malkova, *Izv. USSR Acad. Sciences, Non-organ. Mater* 11 (1975) 2006.
- [25] S.A. Dembovsky and N.P. Lazhnaya, *Sov. J. Non-Organ. Chem.* 9 (1964) 660.
- [26] F.F. Alyakshiev, E.I. Borkach, V.P. Ivanitsky, O.V. Luksha and Yu.Yu. Firtsak, in: *Proc. Sov. Quantum Electronics*, Vol. 30 (Naukova dumka, Kiev, 1986) p. 69.
- [27] P. Vashishta, K. Kalia Rajiv and I. Ebbsjo, *Phys. Rev. B* 39 (1989) 6034.
- [28] P. Viscor, *J. Non-Cryst. Solids* 101 (1988) 156.
- [29] A.C. Wright, R.N. Sinclair and A.J. Leadbetter, *J. Non-Cryst. Solids* 71 (1985) 295.